Stopped-Flow, Laser-Flash Photolysis Studies on the Reactions of CO and O_2 with the Cytochrome *caa*$_3$ Complex from *Bacillus subtilis*: Conservation of Electron Transfer Pathways from Cytochrome *c* to O_2[†]

Bruce C. Hill

Department of Biochemistry, Queen's University, Kingston, Ontario K7L 3N6, Canada

Received October 18, 1995; Revised Manuscript Received March 5, 1996[⊗]

ABSTRACT: The reaction of CO and O_2 with fully reduced cytochrome *caa*$_3$ from *Bacillus subtilis* has been studied by rapid reaction spectrophotometry. The fully reduced *caa*$_3$ complex reacts with CO to give a spectrum that is characteristic of formation of ferrocytochrome a_3−CO. This adduct is photosensitive, and its recombination rate is proportional to CO concentration with a bimolecular value of $1.2 \times 10^5 M^{-1}$ s^{-1}. When the CO compound of the reduced complex is exposed to O_2, the rate of oxidation proceeds at 0.1 s^{-1}, which is assigned as the CO off rate. These kinetic constants give an equilibrium dissociation constant for the CO complex of 0.83 μM. Photolysis of the CO adduct in the presence of O_2 reveals three reaction phases over the first 3 ms and an additional phase on the second time scale. A kinetic model is proposed in which fully reduced oxidase first combines with O_2 and then electron transfer commences from both cytochrome *a* and a_3, followed rapidly by electron input from Cu_A and the cytochrome *c* domain. An equivalent kinetic model has been used to account for the reactivity of mammalian cytochrome *c* oxidase in its electrostatic complex with soluble cytochrome *c* [Hill, B. C., (1994) *J. Biol. Chem. 269,* 2419−2425]. However, unlike the mitochondrial complex, the reactivity of cytochrome *c* in the *B. subtilis caa*$_3$ complex is unaffected by ionic strength. Thus the cytochrome *c* moiety in the *B. subtilis caa*$_3$ complex seems to be fixed in a reactive orientation by its covalent association with the rest of the oxidase complex. The pathway of electron transfer from cytochrome *c* to O_2 appears very well conserved from *B. subtilis* to the mammalian respiratory chain, making the *B. subtilis* protein a good model to probe intersite electron transfer within the cytochrome *c*−cytochrome oxidase complex.

Cytochrome *c* oxidase is the terminal member of the mitochondrial respiratory chain and catalyzes electron transfer from reduced cytochrome *c* to O_2. The oxidase complex is also capable of conserving free energy, and it does so by coupling the generation of a transmembrane proton gradient to the exergonic electron transfer reaction (Wikström & Babcock, 1992). Sequence analysis of the genes encoding the subunits of cytochrome oxidase from a large number of aerobic organisms has revealed a cytochrome oxidase family with two different subclasses (Trumpower & Gennis, 1994). One subclass includes those, such as the mitochondrial oxidase, that oxidize cytochrome *c*, whereas the second group are those that use quinol as reducing substrate, such as the cytochrome *bo* complex from *Escherichia coli*.

Members of the oxidase family share a high degree of homology between subunits I and II, and these core subunits have now been shown definitively to house the redox active sites of the enzyme (Tsukihara et al., 1995; Iwata et al., 1995). Subunit I provides the histidines which act as inner sphere ligands to cytochrome *a* and for the binuclear cytochrome a_3−Cu_B center. It is within the structure of subunit II that the underlying functional distinction between the two subclasses is to be found. The cytochrome *c* oxidases have the amino acids within the primary sequence of subunit II that are inner sphere ligands to the binuclear, mixed-spin Cu_A center. This center acts as the intermediary electron transfer site for receiving electrons from cytochrome *c* and passing them to cytochrome *a* (Hill 1991, 1994). In subunit II of quinol oxidases the Cu_A center ligands are not conserved, and presumably a site for electron exchange with the more hydrophobic quinol molecule has taken over the electron entry role fulfilled by Cu_A in the cytochrome *c* oxidases.

The aerobic bacterium *Bacillus subtilis* expresses two members of the cytochrome oxidase superfamily (Lauraeus et al., 1991; Hill et al., 1993). There is a cytochrome *aa*$_3$ complex that is a quinol oxidase and a cytochrome *caa*$_3$ complex that is a cytochrome *c* oxidase. The quinol oxidase like the cytochrome *bo* complex from *E. coli* lacks the Cu_A center (Henning et al., 1995). The cytochrome *caa*$_3$ complex has the necessary ligands to form Cu_A within subunit II and an additional C-terminal extension to subunit II. This extension has the signal sequence for covalent attachment of heme C, and the overall homology is such that it probably folds into a distinct cytochrome *c* domain. It is the role of this domain in the electron transfer reaction of the *caa*$_3$ oxidase that is the focus of this paper.

Cytochrome *c* oxidase as found in the mitochondrial respiratory chain forms a transitory complex with cytochrome *c* in the process of electron exchange between the two proteins. The complex is proposed to be mediated largely by electrostatic interactions between lysine residues on the surface of cytochrome *c* (Ferguson-Miller et al., 1978) and acidic residues on the surface of subunit II of the oxidase (Millett et al., 1983; Witt et al., 1995). This complex is quite stable at low ionic strength and has allowed electron

[†] This research was supported by an operating grant from the Natural Sciences and Engineering Research Council (Canada).

[⊗] Abstract published in *Advance ACS Abstracts,* April 15, 1996.

S0006-2960(95)02486-X CCC: $12.00

exchange between cytochrome *c* and cytochrome oxidase to be studied without the complication of binding and dissociation (Hill & Greenwood, 1984). These studies have revealed the role of Cu_A as the initial electron acceptor from reduced cytochrome *c* to the oxidase complex (Hill, 1991). The elements of the transient complex between cytochrome *c* and cytochrome oxidase of the mitochondrial respiratory chain are found stabilized in a covalent complex in the *B. subtilis* respiratory chain. The results presented in this paper show that the electron transfer activity of cytochrome *c* in the covalent *B. subtilis* complex is nearly identical to that found in the ionically stabilized, mitochondrial complex. This result leads to the conclusion that there is a high degree of functional homology in these two systems that arises from their conserved structures. The *B. subtilis caa*$_3$ complex is a good model of the reactive complex formed transiently between cytochrome *c* and cytochrome oxidase in mitochondria, and the pathway of electron transfer from cytochrome *c* to O_2 appears to be well conserved.

EXPERIMENTAL PROCEDURES

The cytochrome *caa*$_3$ complex was purified from *B. subtilis* plasma membranes as described by Henning et al., (1995). In the last stage of column chromatography the protein was extensively washed with lauryl maltoside and eluted in lauryl maltoside containing buffer. The purified protein contained subunits I and II with a heme to protein ratio in the range of 18−21 nmol of heme A/mg of protein. The cytochrome *caa*$_3$ concentration was determined using a reduced−oxidized extinction coefficient of 25.2 mM^{-1} cm^{-1} at 604−630 nm (Lauraeus et al., 1991). The reduced-oxidized extinction coefficient of the cytochrome *c* moiety is determined on this basis to be 32.5 mM^{-1} cm^{-1} at 550−540 nm. The extinction coefficient for the cytochrome *c* domain is unusually high, but we do not find contamination from free cytochrome *c* in our preparation. Moreover, the extinction coefficients are supported by pyridine hemochromagen determinations performed as described by Berry and Trumpower (1987) and are consistent with the other spectrum of this complex published in the literature (Lauraeus et al., 1991). Protein concentration was determined by the method of Smith et al. (1985) using bovine serum albumin as standard. In the single-turnover reactions the buffer was either sodium phosphate or Tris containing 0.5 mg/mL lauryl maltoside.

The kinetic spectrometer used here was identical to that described by Hill (1991, 1994). Rapid mixing was performed with a three-syringe system from Bio-Logic, and the path length of the observation cuvette was 1 cm. Kinetic absorption data were collected using a Philips digital oscilloscope (Model PM3323) under the control of Asystant GPIB data processing package. Initial kinetic analysis was performed using Asystant and a multiexponential expression of the form shown below.

$$\Delta A = A(\exp -k_1 t) + B(\exp -k_2 t) + C(\exp -k_3 t) + D(\exp -k_4) + E$$

ΔA is the overall absorbance change observed at a particular wavelength, and the terms *A*, *B*, *C*, and *D* are preexponential factors that represent the absorbance contribution of the kinetic species changing at the observed rates k_1, k_2, k_3, and k_4, respectively. The term *E* allows for the baseline absorbance to be fit independently. Numerical analysis of the system of differential equations derived from Scheme 1 gives the time course for each intermediate as shown in Figure 5A,C. The intermediates were then assigned extinction coefficients to generate the simulation of the observed absorbance changes. The numerical analysis was done in Scientist.

RESULTS

The reaction of the cytochrome *caa*$_3$ complex with O_2, as with other members of the cytochrome oxidase family, is very rapid and beyond the resolution of conventional rapid mixing. In this work the method of stopped-flow, flash-photolysis has been used to characterize the transient absorbance changes that occur when the fully reduced form of cytochrome *caa*$_3$ reacts with O_2. In this approach the CO complex of the reduced enzyme is mixed with O_2, and the CO is removed by a laser flash that is of sufficient energy to cause complete photolysis of the CO adduct. The fully reduced, unliganded oxidase then reacts with O_2. Figure 1 shows optical difference spectra of the states of the cytochrome *caa*$_3$ complex used in this work. Peaks are found at 416, 520, and 550 nm in the reduced-oxidized difference spectrum (see Figure 1A), typical of reduced cytochrome *c*, and at 445 and 604 nm that are typical of reduced cytochromes *a* and *a*$_3$. The reduced spectrum is identical using the pseudosubstrate, sodium ascorbate plus TMPD, or the strong reductant sodium dithionite. This result indicates that there is little sluggishly reactive enzyme in this preparation.

Figure 1B is the difference spectrum induced by CO addition to the fully reduced cytochrome *caa*$_3$ complex. This spectrum has the form and intensity characteristic of CO ligation to ferrocytochrome *a*$_3$. Panel C shows the visible region in more detail to illustrate that there is no indication of CO ligation to ferrocytochrome *c*. Lack of CO reactivity of the cytochrome *c* moiety in the cytochrome *caa*$_3$ complex implies that the axial ligand positions to heme C are stably occupied similar to the native state of mitochondrial cytochrome *c*. The open circles on this figure are obtained from the transient absorbance induced upon laser photolysis of this complex. The concurrence of the photolysis and ground state difference spectra indicates that, on this time scale, there are no additional states induced in the enzyme by the photolysis reaction itself. The time response of the detector in the system used here is 0.7 μs, and so we do not anticipate being able to resolve the small, rapid signals reported by Georgiadis et al. (1994) with the bovine *aa*$_3$−CO complex.

CO Reaction Kinetics. The kinetics of the reaction of the cytochrome *caa*$_3$ complex with CO are illustrated in Figure 2. Panel A shows transient absorbance changes observed upon photolysis of the CO adduct of fully reduced *caa*$_3$ at 610 and 590 nm. The time courses begin with the immediate change induced by photolysis followed by the slower reaction of CO recombination that leads to return of the prephotolytic absorbance level. The time courses at all wavelengths and all CO concentrations are well fit by a single-exponential time course. The dependence of the observed rate of recombination derived from the single-exponential analysis is linear when plotted as a function of CO concentration over the range from 20 to 160 μM. The second order rate of reaction of the cytochrome *caa*$_3$ complex with CO is 1.2 ×

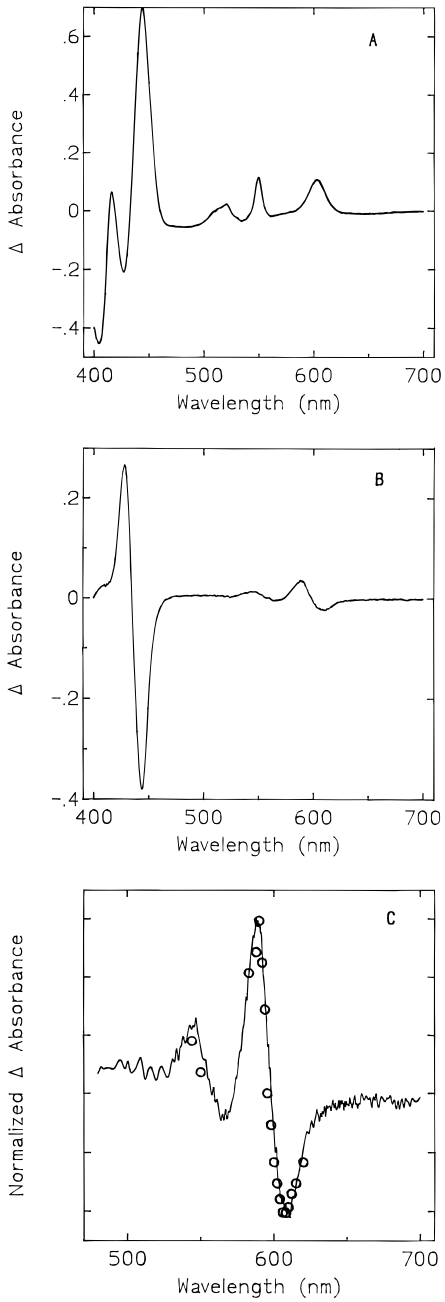

FIGURE 1: Optical difference spectra of the cytochrome caa_3 complex from *B. subtilis*. (A) Reduced−oxidized spectrum. The enzyme was reduced with 4 mM sodium ascorbate plus 80 μM TMPD, and the spectrum was recorded using the oxidized enzyme as reference. The buffer was 10 mM sodium phosphate pH 7.4 with 0.5 mg/mL lauryl maltoside, and the enzyme concentration was 4.35 μM. (B) Reduced, plus CO-reduced. CO was added to the fully reduced enzyme to a concentration of 1 mM, and the spectrum was recorded using the reduced enzyme as reference. (C) Comparison of transient and ground state CO difference spectra in the visible region. The solid line is the same spectrum as panel B shown on an expanded scale with the *Y*-axis normalized to the value of the peak to trough absorbance at 590−610 nm. The open circles are the normalized transient absorbance values observed upon photolysis of the CO adduct.

10^5 M^{-1} s^{-1}. Over the limited CO concentration range used here we do not see evidence for saturation kinetics as reported for bovine oxidase at CO pressures higher than one atmosphere (Einarsdóttir et al., 1993). Panel B shows the time course of the reaction of the cytochrome caa_3−CO complex with O_2 in the dark. The rate of reaction is similar at 445 and 604 nm with a single-exponential form giving an

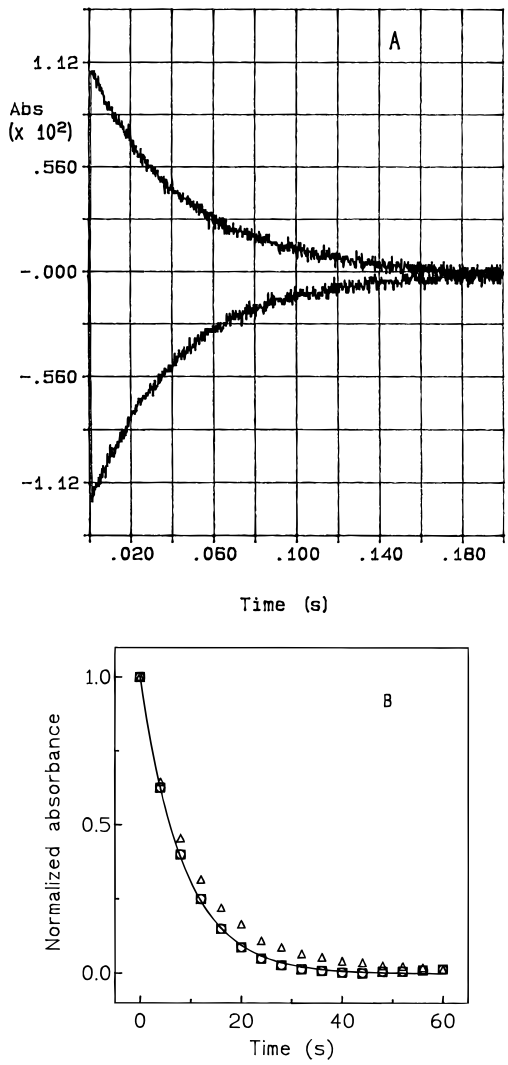

FIGURE 2: Kinetics of the reaction of the cytochrome caa_3 complex with CO. (A) Transient absorbance changes upon photolysis of CO from reduced cytochrome caa_3. The top trace was recorded at 610 nm and the bottom trace at 590 nm. The CO concentration was 160 μM- and the other conditions were identical to those outlined in the legend to Figure 1. (B) O_2 reaction of CO-bound, reduced cytochrome caa_3. The enzyme was equilibrated with N_2 and incubated with 1 mM sodium ascorbate until full reduction was obtained. The N_2 atmosphere was then replaced with CO to obtain the fully reduced CO adduct. The CO atmosphere was then displaced with O_2 and the cuvette thoroughly mixed. The reaction was recorded by taking the spectrum from 400 to 700 nm every 2 s. Absorbance difference time courses are shown at 444−460 nm (□), 604−630 nm (○), and 550−540 nm (△). The smooth line is a single-exponential fit to the data at 604 and 444 nm. The buffer conditions were the same as those given in the legend to Figure 1, and the enzyme concentration was 9.05 μM.

observed first-order value of 0.1 s^{-1}. This rate is assigned to the dissociation of CO from ferrocytochrome a_3 and is observed to limit the reaction with O_2 of cytochrome aa_3, observed at 604 and 445 nm. The oxidation of cytochrome *c*, monitored at 550 nm, proceeds with a similar rate. This is consistent with the view that the reaction between cytochrome *c* and O_2 is mediated by cytochrome aa_3 as would be expected for this complex in its native state. These rates for CO association and dissociation give an equilibrium dissociation constant, K_D, of 0.83 μM. This value defines a somewhat weaker binding of CO to the cytochrome caa_3 complex relative to that found for bovine heart cytochrome oxidase of 0.3 μM (Gibson & Greenwood, 1963), and most

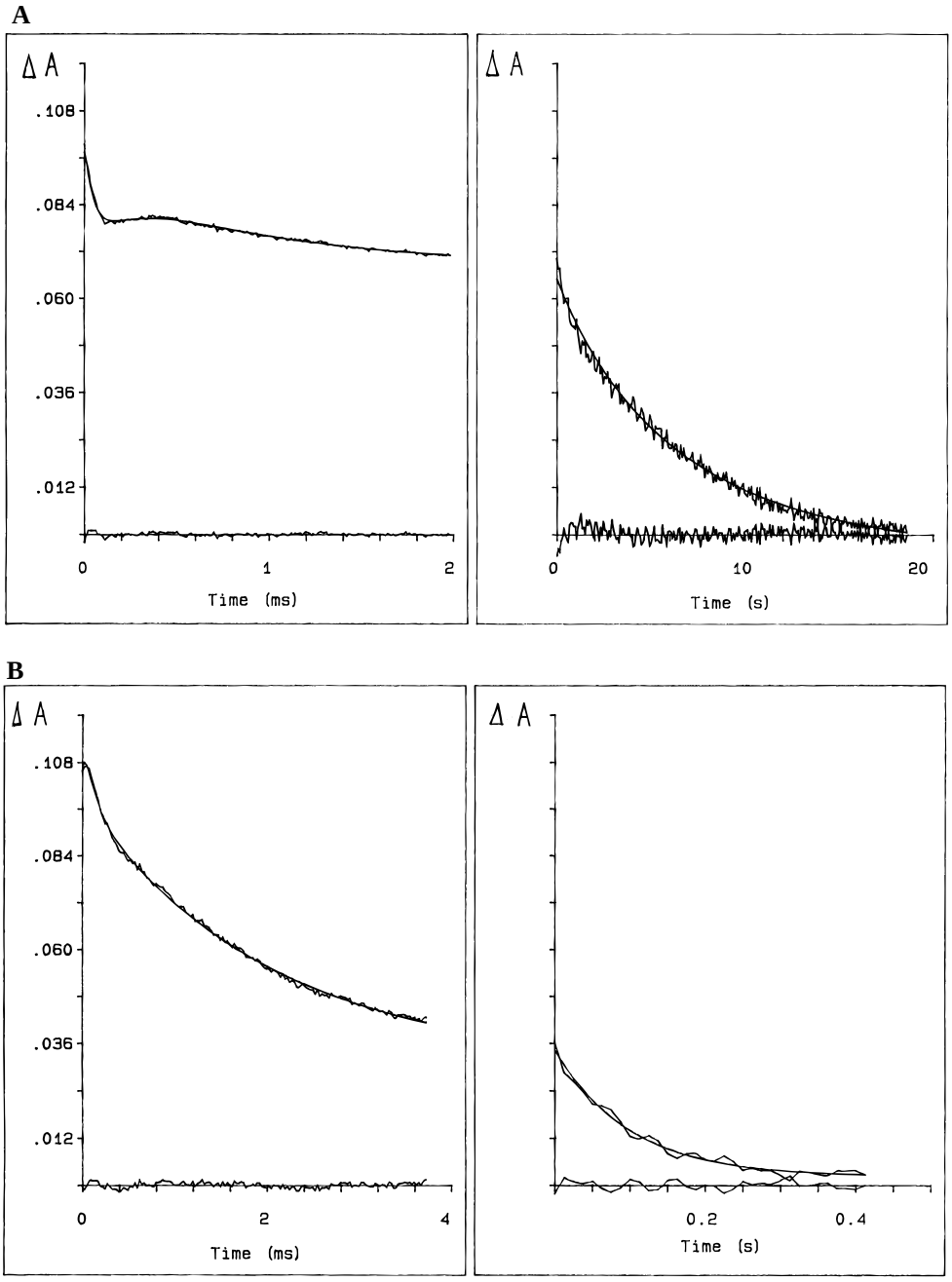

FIGURE 3: Flow-flash photolysis reaction of cytochrome *caa*$_3$ with O_2. The final concentration of enzyme was 11 μM, and the O_2 concentration was 400 μM. The buffer was 50 mM Tris, pH 7.8, with 1 mg/mL lauryl maltoside. The enzyme was reduced with 2.5 mM sodium ascorbate plus 2.5 μM TMPD, prior to addition of 1 atmosphere CO and transfer to the drive syringe of the stopped-flow. The laser flash was triggered 5 ms after the flow-stopped, and traces commence following the CO dissociation process. The left and right panels in panel A are on the same absorbance scale at 604 nm but on two different time scales. Panel B also shows two panels on the same absorbance scale at 550 nm and two different time scales. The smooth lines through the data are multiexponential fits, and the plots along the *x*-axis show the residuals between the fitted and observed data.

of this difference is found in the more rapid dissociation of CO from the *B. subtilis* oxidase.

O_2 Reaction. Although the CO dissociation rate from the cytochrome *caa*$_3$ complex is about five times faster than its mitochondrial counterpart it is still accessible to the method of flow-flash photolysis. Figure 3 illustrates the reaction of the cytochrome *caa*$_3$ complex with 400 μM O_2, following photolysis of CO, at 604 and 550 nm. This concentration of O_2 was chosen because in work with mitochondrial cytochrome oxidase it gives kinetic discrimination of the multiphase reaction (Hill, 1991). At 604 nm the reaction begins with an initial rapid decrease in absorbance followed by a partial reversal and then a further decrease on a 2 ms time scale. Further absorbance decrease is on a time scale of 20 s. At 550 nm the time course begins with a lag followed by two phases of absorbance decline within the first 2 ms. Further absorbance decline at 550 nm takes place in the next 0.5 s. The initial absorbance changes at both wavelengths over the first 2 ms can be fit by a triple-exponential rate law, and the smooth lines through the data are the fitted curves. The residual difference between the fitted and observed data is shown plotted at the bottom on each panel. The slower changes can be fit by an additional, fourth, exponential process. The values of the observed rate constants and the corresponding absorbance magnitudes are given in Table 1. At 604 nm about 35% of the reaction is

Table 1: Kinetic Parameters Derived from Multiexponential Analysis of the Reaction of Fully Reduced Cytochrome *caa*$_3$ with O_2

	604 nm		550 nm	
phase	k_{obs} (s^{-1})	ΔA	k_{obs} (s^{-1})	ΔA
1	2.2×10^4	0.028	2.2×10^4	−0.010
2	5.8×10^3	−0.012	6.0×10^3	0.020
3	640	0.021	480	0.068
4	0.2	0.07	11.5	0.032

[a] The values reported for the observed rates and ΔA were obtained from fitting a multiexponential expression of the type shown in Experimental Procedures to the observed data in Figure 3. The error in these values is in the range of 15%.

complete after 3 ms, whereas at 550 nm 73% of the reaction is complete at 3 ms. The initial lag observed at 550 nm is fit as an absorbance increase in the multiexponential analysis. Although these observed rates do not correspond to elementary rate constants, they do form the starting point for the mechanistic modeling carried out below. The rates at the two wavelengths do differ substantially over the very slow phase. The faster rate for the fourth phase of cytochrome *c* oxidation probably reflects the more rapid equilibration of cytochrome *c* with other oxidized components within the same oxidase molecule compared to slower intermolecular shuffling of electrons between different enzyme molecules that limits oxidation of cytochrome *a*.

Figure 4 shows the effect of ionic strength on the O_2 reaction of the cytochrome *caa*$_3$ complex. This figure concentrates on the initial rapid phases of the reaction and is shown at three different wavelengths. The reactions are very similar at high and low ionic strengths at all three wavelengths. The same result was obtained when sodium phosphate was used as the ionic species and leads to the conclusion that ionic strength does not affect the association of the cytochrome *c* domain with its reactive partner in the cytochrome *caa*$_3$ complex. In these time courses the traces are set to zero absorbance at the pre-flash level, i.e., the absorbance of the CO adduct. The absorbance at 604 nm begins with an immediate absorbance increase due to dissociation of CO, and this is consistent with the initial absorbance decline seen at 590 nm. At 550 nm there is a large interference from the laser flash, which is centered at 535 nm and is seen as an absorbance decrease, after which the absorbance returns to the preflash level. The absorbance at 604 nm following CO photolysis follows the same pattern seen in Figure 3 above. In this case, however, the second phase of the oxygen reaction is more apparent, and the third phase is less prominent than the sample shown in Figure 3. This result arises partially from the higher O_2 concentration used in Figure 4 and from a faster rate of electron transfer to re-reduce cytochrome *a*. The latter effect is reflective of the preparation to preparation variation in these values. The pattern at 550 nm is also similar to that shown in Figure 3 except that the initial faster phase takes more of the reaction time course. At 590 nm the absorbance initially declines due to CO photolysis; however, the extent of this phase is diminished in the presence of O_2, and at higher time resolution (not shown) it is apparent that a species absorbing at 590 nm replaces the CO complex as it is photolyzed. Presumably, this is the O_2 adduct of ferrocytochrome a_3. The absorbance profile at 590 nm then follows the form observed at 604 nm.

Mechanistic Model of the O_2 Reaction. Scheme 1 shows a proposal for the reaction sequence for the single turnover of fully reduced cytochrome *caa*$_3$ with O_2. This model was developed for the single turnover reaction of bovine heart cytochrome oxidase (Hill, et al., 1986; Hill, 1991) and has been extended to the electrostatic complex between cytochrome *c* and cytochrome oxidase (Hill, 1994). The *caa*$_3$ complex is represented as a polygon with five sections representing the five redox centers of the enzyme. The sequence begins with fully reduced, unliganded cytochrome *caa*$_3$ (i.e., intermediate 0), the species produced following photolysis in the flow-flash experiment. The five compartments in the polygon are labeled in intermediate 0, and thereafter only their oxidation state relative to their state in the fully reduced enzyme is indicated.

The fully reduced enzyme is shown to react with O_2 to yield an oxy form of cytochrome oxidase, which is represented as O_2 bound to ferrocytochrome a_3. There is evidence from transient kinetic studies on bovine heart oxidase in the near infrared region that the initial complex has O_2 bound to Cu_B from where it transfers to cytochrome a_3 (Oliveberg & Malmström, 1992). We have not had enough enzyme to explore this spectral region, but the inclusion of this intermediate does not change the results of the modeling presented here. Intermediate I formation is followed by rapid electron transfer from cytochromes *a* and a_3 to give intermediate II. A peroxy level is assumed for O_2 in intermediate II, although conclusive evidence for the state of this intermediate is lacking [see Babcock & Wikström (1992) and Proshlyakov et al. (1994)]. Proton uptake is proposed to occur at two stages, in the transition from intermediate III to IV and IV to Vb. This is consistent with experimental measurements of ΔpH during this reaction (Oliveberg et al., 1991). Oxygen bond scission is proposed to occur in the step from IV to Vb and renders this step essentially irreversible.

Following formation of the peroxy species (i.e., Intermediate II) intramolecular electron transfer is proposed to occur from Cu_A to re-reduce cytochrome *a*, and this largely accounts for the absorbance increase seen at 604 nm. Cytochrome *c* is then able to exchange electrons with the Cu_A center in a reaction which is proposed to be extremely rapid (see below) and allows cytochrome *c* oxidation to parallel the redox state of Cu_A. Cytochrome *a* is then reoxidized in a reaction which only goes to partial completion after a few milliseconds. At this stage there is rapid equilibrium between one-electron reduced states that decays to the fully oxidized level on a time scale of seconds, presumably through a mechanism involving intermolecular electron exchange.

The simulated time courses of the intermediates generated from Scheme 1 are shown in Figure 5. The time courses of the intermediates were determined by numerical integration of the system of linear differential equations derived from Scheme 1 using the rates listed in Table 2. The rates for the initial electron exchange from cytochrome *a* to cytochrome a_3 (i.e., k_2 and k_{-2}) and for electron exchange from Cu_A to cytochrome *a* (i.e., k_3 and k_{-3}) in Table 2 are consistent with measurements from perturbed equilibrium experiments [e.g., Oliveberg and Malmström (1991)]. The rates assigned for electron transfer from cytochrome *c* to Cu_A (i.e., k_4 and k_{-4}) are consistent with measured values for electron input at this site [e.g., Pan et al. (1993)]. Figure 5A depicts the

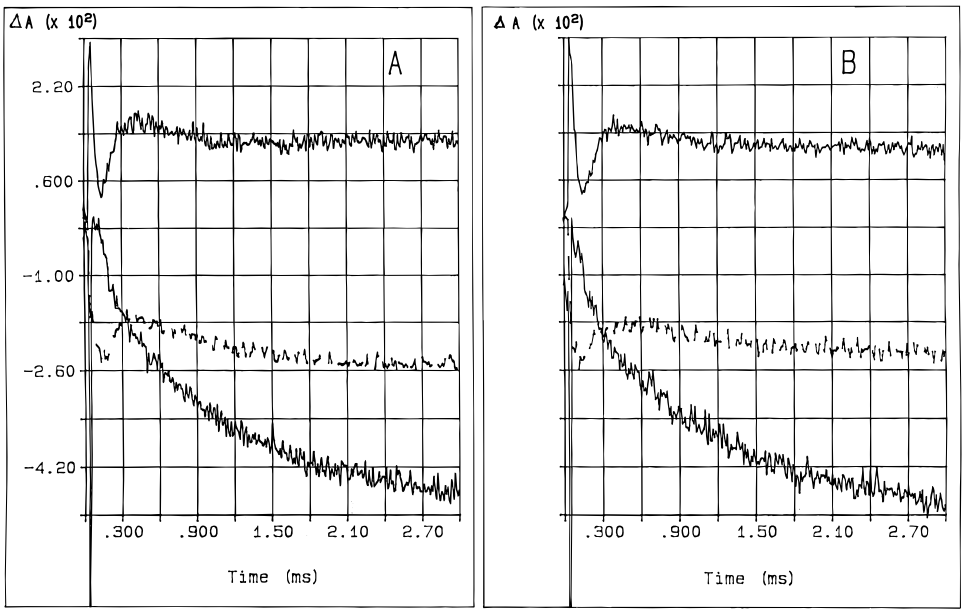

FIGURE 4: Flow-flash photolysis reaction of cytochrome *caa*$_3$ at low and high ionic strengths. The enzyme concentration was 9.2 μM, and the O_2 concentration was 600 μM. In panel A the buffer was 50 mM Tris, pH 7.8, with 0.5 mg/mL lauryl maltoside. The conditions were the same in panel B except 265 mM sodium chloride was added to the buffer. The traces are each set to zero ΔA at the level prior to photolysis. The upper solid trace in each panel was recorded at 604 nm, the lower solid trace at 550 nm, and the dashed line trace at 590 nm. The two sets of traces are presented on the same absorbance scale.

Scheme 1. Sequence of Intermediates during the Reaction of the Fully Reduced Cytochrome *caa*$_3$ Complex with O_2

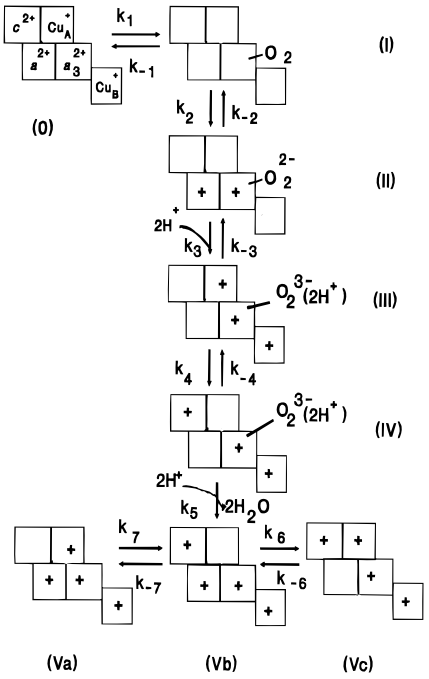

time courses of intermediates 0−IV over the first 0.5 ms. The values of the elementary rates are similar to those used in simulations of the O_2 reaction of mitochondrial oxidase and the cytochrome *c*−cytochrome *aa*$_3$ complex (Hill, 1994) with the added feature that all the initial steps are reversible (Verkhovsky et al., 1994). The fourth electron into O_2 (i.e., k_5) is retained as an irreversible step and is probably limited by a different factor, possibly O−O bond cleavage or H^+ binding, than the initial heme oxidation step. Absorbance changes were calculated using the relative extinction coefficients in Table 2 for each of the intermediate species. Figure 5B shows the simulated absorbance changes at 550 and 604 nm over the first 0.5 ms. There is an initial rapid decline at 604 nm due a combination of the formation of oxyferrocytochrome a_3 and rapid electron transfer to bound oxygen from both cytochrome *a* and a_3. The absorbance at 604 nm then increases from 100 to 300 μs due to intramolecular electron transfer from Cu_A to cytochrome *a* and to the formation of a peroxy species at cytochrome a_3. The absorbance time course at 550 nm begins with a lag as the oxidation of cytochrome *c* does not commence until the appearance of intermediate IV. About 30% of cytochrome *c* is oxidized in the first phase.

The results of the simulation run out to 3 ms are shown in Figure 5C,D. Panel C traces the concentrations of intermediates IV, Va, b, and c. Intermediate IV rises to a maximum at 0.5 ms and then decays over the next few ms. The family of intermediates V rises slowly out to 3 ms with intermediate Vc dominating at the end of the simulation. This intermediate has cytochrome *a* reduced and accounts for the high level of absorbance reached at 3 ms in the experimental trace in Figure 4. Panel D shows the simulated absorbance time course out to 3 ms. The absorbance at 604 nm declines only slightly after 0.5 ms, whereas there is a substantial phase of cytochrome *c* oxidation that takes place between 0.5−3 ms. Finally, it is important to note that the model presented here is not exclusive of others, and the values for the rates and extinction coefficients are not a unique solution. However, the simulation allows the test of whether the proposed model can reasonably reproduce the experimental data. As more data are available, the model can be refined.

DISCUSSION

Interprotein complexation is an important step in many metabolic processes, and particularly in electron transfer reactions involved in aerobic respiration. Mitochondrial cytochrome *c* forms a transient complex with cytochrome *c* oxidase during the transfer of electrons to O_2. In the *B. subtilis* respiratory chain this interaction is stabilized by the incorporation of a cytochrome *c* domain into the sequence

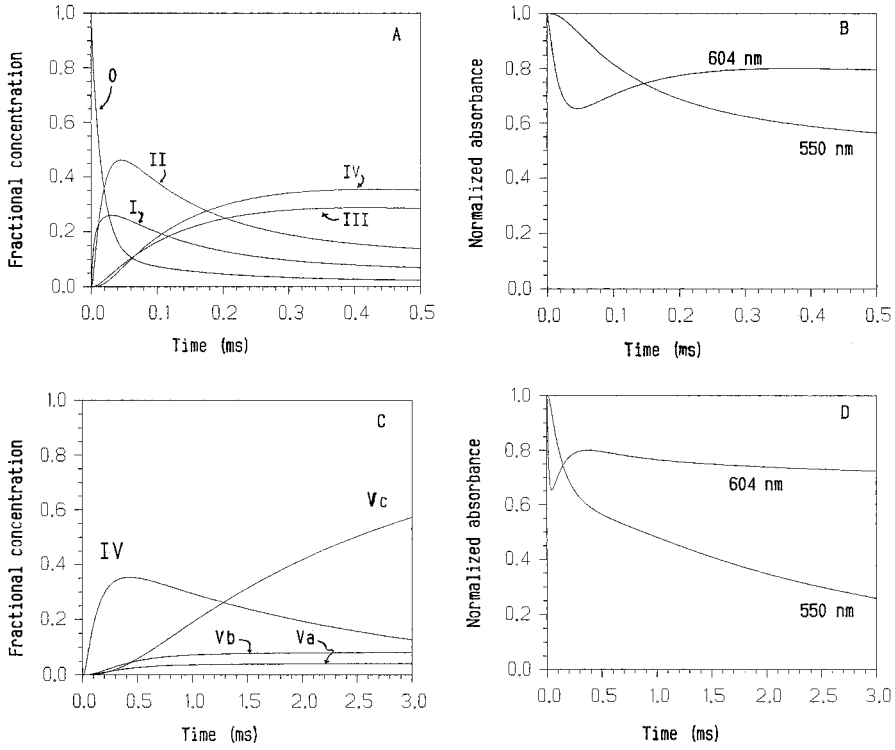

FIGURE 5: Kinetic simulation of the single turnover of reduced cytochrome *caa*$_3$ with O_2. (A) Time courses of intermediates O−IV over the first 0.5 ms according to scheme 1 and using the elementary rates given Table 2. The *Y*-axis refers to the relative concentration of the enzyme. The simulation begins with all the enzyme in the fully reduced state. (B) Simulated absorbance changes at 550 and 604 nm over the first 0.5 ms using the relative extinction coefficients given in Table 2. (C) Time courses of intermediates IV−Va,b,c out to 3 ms. The *Y*-axis is the sane as in panel A. (D) Simulated absorbance changes at 604 and 550 nm out to 3 ms.

Table 2: Elementary Rate Constants and Relative Extinction Coefficients Used for Modeling Transient Absorbance Changes in the O_2 Reaction of Cytochrome *caa*$_3$

			relative ΔE	
	rates	intermediate	604 nm	550 nm
k_1	1×10^8 M^{-1} s^{-1}	O	1	1
k_{-1}	2×10^4 s^{-1}	I	0.9	1
k_2	2×10^5 s^{-1}	II	0.3	1
k_{-2}	1×10^5 s^{-1}			
k_3	1×10^4 s^{-1}	III	1.2	1
k_{-3}	4×10^3 s^{-1}			
k_4	1×10^5 s^{-1}	IV	0.8	0
k_{-4}	8×10^4 s^{-1}			
k_5	1×10^3 s^{-1}	Vb	0	0
k_6	1×10^4 s^{-1}	Vc	0.8	0
k_{-6}	5×10^2 s^{-1}			
k_7	1×10^5 s^{-1}	Va	0	1
k_{-7}	5×10^4 s^{-1}			

of subunit II of the oxidase to produce the cytochrome *caa*$_3$ complex. This paper presents data on the reaction of this covalently stabilized complex with O_2 which demonstrates that it exhibits reactivity almost indistinguishable from the ionically stabilized complex formed between soluble, mitochondrial cytochrome *c* and cytochrome oxidase. It is proposed, therefore, that the structure of the mitochondrial protein−protein complex is highly similar to the covalently stabilized *B. subtilis* complex. The site on subunit II of mitochondrial oxidase involving several conserved acidic residues (Millett et al., 1983) is near the Cu_A center (Tsukihara et al., 1995) and is the predominant site for electron exchange between cytochrome *c* and cytochrome oxidase. Moreover, the electron transfer pathway from cytochrome *c* to O_2 found in the covalently stabilized *B. subtilis* oxidase has been conserved in the electron exchange complex formed between the individual, mammalian mitochondrial proteins.

Subunit II of the *B. subtilis* oxidase is homologous with other members of the cytochrome oxidase family (Saraste et al., 1991a). It is predicted from hydropathy analysis to have two transmembrane α-helices at the N-terminal end. This is followed by an aqueous domain which possesses a cupredoxin motif and houses the amino acids that form the Cu_A center (Saraste et al., 1991b). The subunit II sequence from *B. subtilis* has a further C-terminal extension of about 100 amino acids which has about 45% sequence homology with cytochrome *c*-551 from *Pseudomonas aeruginosa* and is thought to form a cytochrome *c* domain. The kinetic results presented here lead to the conclusion that this cytochrome *c* domain in the *B. subtilis* cytochrome *caa*$_3$ complex functions in an analogous manner to mammalian cytochrome *c* in its electrostatic complex with cytochrome oxidase. The cytochrome *c* domain in the *caa*$_3$ complex appears to be held in the same reactive disposition that is taken up by soluble cytochrome *c* when it forms the transient complex with mitochondrial cytochrome oxidase.

The *B. subtilis* subunit II has also retained in its sequence a number of acidic residues that could mediate tight, electrostatic binding of free cytochrome *c*. However, we know that *B. subtilis caa*$_3$ does not form high affinity complexes with free cytochrome *c* (Hebert and Hill, unpublished result). Presumably, this is because the covalently bound cytochrome *c* domain occupies this site. Perhaps the cytochrome *c* domain retains some flexibility in its interaction within subunit II allowing for changes in the relative position or orientation of the cytochrome *c* domain, mediated by electrostatic forces, and thus altered by ionic strength. The finding reported here that the kinetics of cytochrome *c*

oxidation are not affected by changes in ionic strength makes this possibility unlikely. This result also raises the question as to the mechanism of reduction of the *B. subtilis* caa_3 complex. The mitochondrial complex between cytochrome *c* and cytochrome oxidase is transient because cytochrome *c* must dissociate from cytochrome oxidase to pick up reducing equivalents from the cytochrome bc_1 complex. Since the cytochrome *c* domain in the caa_3 oxidase does not appear to alter its tight interaction with the Cu_A center this suggests an alternative path of electron transfer to the cytochrome *c* heme must be functional in the caa_3 oxidase. This is a question we are pursuing currently.

The similarity between the time courses of the *B. subtilis* caa_3 complex and the mitochondrial complex, and the ability to closely reproduce these time courses with a very similar mechanistic model, suggests that the details of the O_2 reaction are similar. The electron transfer pathways from cytochrome *c* into the oxidase and onto O_2 have been conserved form this prokaryotic oxidase to its mitochondrial counterpart. In addition it is also clear that the entire pattern of the single-turnover reaction of the caa_3 complex is unaltered by ionic strength. This is in contrast to a recent report from Orii et al. (1995) on the cytochrome *bo*−ubiquinol oxidase from *E. coli*. These workers present a profound difference between the O_2 reactivity of cytochrome *bo* prepared in chloride or sulphate containing buffers and ascribe this effect to a specialized role for chloride in the process of intramolecular electron transfer. Such an effect is not seen with the cytochrome caa_3 complex from *B. subtilis* or with bovine cytochrome oxidase (Hill, 1991). The kinetic traces from Orii et al. (1995) could be explained if there is a stoichiometric amount of tightly bound quinol in the sulfate-prepared cytochrome *bo* that is not present in the chloride preparation. This quinol can re-reduce the cytochrome *b* heme in the same manner that has been proposed for Cu_A here and for the mitochondrial oxidase (Hill, 1994).

REFERENCES

Babcock, G. T., & Wikström, M. (1992) *Nature 356*, 301−309.

Berry, E. A., & Trumpower, B. L. (1987) *Anal. Biochem. 161*, 1−15.

Einarsdóttir, Ó., Dyer, R. B., Lemon, D. D., Killough, P. M., Hubig, S. M., Atherton, S. J., López-Garriga, J. J., Palmer, G., & Woodruff, W. H. (1993) *Biochemistry 32*, 12013−12024.

Ferguson-Miller, S., Brautigan, D. L., & Margoliash, E. (1978) *J. Biol. Chem. 253*, 149−159.

Georgiadis, K. E., Jhon, N.-I., & Einarsdóttir, Ó. (1994) *Biochemistry 33*, 9245−9256.

Gibson, Q., & Greenwood, C. (1963) *Biochem. J. 86*, 541−555.

Hill, B. C. (1991) *J. Biol. Chem. 266*, 2219−2226.

Hill, B. C. (1994) *J. Biol. Chem. 269*, 2419−2425.

Hill, B. C., & Greenwood, C. (1984) *FEBS Lett. 166*, 362−366.

Hill, B. C., & Greenwood, C., & Nicholls, P. (1986) *Biochim. Biophys. Acta 853*, 91−113.

Hill, B. C., Vo, L., & Albanese (1993) *Arch. Biochem. Biophys. 301*, 129−137.

Henning, W., Vo, L., Albanese, J., & Hill, B. C. (1995) *Biochem. J. 309*, 279−283.

Iwata, S., Ostermeier, C., Ludwig, B., & Michel, H. (1995) *Nature 376*, 660−669.

Lan, L. P., Hibdon, S., Liu, R. Q., Durham, B., & Millett, F. (1993) *Biochemistry 32*, 8492−8498.

Lauraeus, M., Haltia, T., Saraste, M., & Wikström, M. (1991) *Eur. J. Biochem. 197*, 699−705.

Millett, F., De Jong, K., Paulson, L., & Capaldi, R. A. (1983) *Biochemistry 22*, 546−552.

Oliveberg, M., & Malmström, B. G. (1991) *Biochemistry 30*, 7053−7057.

Oliveberg, M., & Malmström, B. G. (1992) *Biochemistry 31*, 3560−3563.

Orii, Y., Mogi, T., Sato-Watanabe, M., Hirano, T., & Anraku, Y. (1995) *Biochemistry 34*, 1127−1132.

Proshlyakov, D. A., Ogura, T., Shinzawa-Itoh, K., Yoshikawa, S., Appelman, E. H., & Kitagawa, T. (1994) *J. Biol. Chem. 269*, 29385−29388.

Saraste, M., Holm, L., Lemieux, L., Lübben, M., & van der Oost, J. (1991a) *Biochem. Soc. Trans. 19*, 608−612.

Saraste, M., Metso, T., Nakari, T., Jalli, T., Lauraeus, M., & van der Oost, J. (1991b) *Eur. J. Biochem. 195*, 517−525.

Smith, P. K., Krohn, R. I., Hermanson, G. T., Mallia, A. K., Gartner, F. H., Provenzano, M. D., Fujimoto, E. K., Goeke, N. M., Olson, B. J., & Klenk, D. C. (1985) *Anal. Biochem. 150*, 76−85.

Trumpower, B. L., & Gennis, R. B. (1994) *Annu. Rev. Biochem. 63*, 675−716.

Tsukihara, T., Aoyama, H., Yamashita, E., Tomizaki, T., Yamaguchi, H., Shinzawa-Itoh, K., Nakashima, R., Yaono, R., & Yoshikawa, S. (1995) *Science 269*, 1069−1074.

Verkhovsky, M. I., Morgan, J. E., & Wikström, M. (1994) *Biochemistry 33*, 3079−3086.

Witt, H., Zickerman, V., & Ludwig, B. (1995) *Biochim. Biophys. Acta 1230*, 74−76.

BI952486F